



A population pharmacokinetic/toxicity model for the reduction of platelets during a 48-h continuous intravenous infusion of the histone deacetylase inhibitor belinostat

Cody J. Peer¹ · Oliver M. Hall¹ · Tristan M. Sissung¹ · Richard Piekarz² · Sanjeeve Balasubramaniam³ · Susan E. Bates⁴ · William D. Figg^{1,5}

Received: 13 March 2018 / Accepted: 21 June 2018 / Published online: 27 June 2018

© This is a U.S. government work and its text is not subject to copyright protection in the United States; however, its text may be subject to foreign copyright protection 2018

Abstract

Purpose Belinostat is a second-generation histone deacetylase inhibitor (HDI) predominantly metabolized by UGT1A1-mediated glucuronidation. Two common polymorphisms (*UGT1A1**28 and *UGT1A1**60) were previously associated with impaired drug clearance and thrombocytopenia risk, likely from increased drug exposure. This latter phenomenon has been observed with other HDIs such as abexinostat, panobinostat, romidepsin, and vorinostat. It was the intention of this brief report to expand a population pharmacokinetic (PPK) model to include a pharmacodynamic (PD) model describing the change in platelet levels in patients with cancer administered belinostat as a 48-h continuous intravenous infusion, along with cisplatin and etoposide.

Methods The PPK/PD model developed here introduced an additional rate constant to a commonly used mechanistic myelosuppression model to better describe the maturation of megakaryocytes into platelets before degradation and a feedback mechanism. The model employed a proportional error model to describe the observed circulating platelet data.

Results Several covariates were explored, including sex, body weight, *UGT1A1* genotype status, liver, and kidney function, but none significantly improved the model. Platelet levels rebounded to baseline within 21 days, before the next cycle of therapy. Simulations predicted that higher belinostat drug exposure does cause lower thrombocyte nadirs compared to lower belinostat levels. However, platelet levels rebound by the start of the next belinostat cycle.

Conclusions This model suggests a q3week schedule allows for sufficient platelet recovery before the next belinostat infusion is optimal.

Keywords Clinical pharmacology · Oncology · Pharmacokinetics · Thrombocytopenia

Introduction

Histone acetylation is associated with numerous mechanisms that induce cancer cell death, and is regulated by histone acetyl transferases and histone deacetylases. Inhibition of histone deacetylases can induce greater histone acetylation and has thus become a widely studied area of oncology

therapy. Belinostat is a second-generation histone deacetylase inhibitor (HDI) that is FDA approved as a 30-min intravenous infusion of 1000 mg/m² given daily on days 1–5 of a 21-day cycle to treat relapsed/refractory peripheral T-cell lymphoma (Beleodaq[®]). Histone deacetylases are reversibly inhibited upon exposure to belinostat; therefore, a prolonged exposure, and in simultaneous combination with DNA-damaging agents that provide a synergistic cytotoxic effect, has been shown to improve therapeutic response [1–3].

A phase I clinical trial (NCT00926640) infused belinostat over 48 h, along with cisplatin and etoposide, and demonstrated that this combination was safe and effective in patients with small cell lung cancer or other neuroendocrine cancers (39% objective response rate [4]). Belinostat is predominantly metabolized via uridine glucuronyltransferases,

Electronic supplementary material The online version of this article (<https://doi.org/10.1007/s00280-018-3631-7>) contains supplementary material, which is available to authorized users.

✉ William D. Figg
figgw@mail.nih.gov

Extended author information available on the last page of the article

specifically *UGT1A1*, and patients with lower function alleles of *UGT1A1*, namely *UGT1A1**28 (extra TA in promoter region conferring lower expression) and *UGT1A1**60 (−3279 T>G in promoter region conferring lower expression), had slower belinostat clearance [5, 6]. Based on these findings, a population pharmacokinetic (PPK) model was developed that simulated an optimal dose reduction (33%) for patients that are considered impaired *UGT1A1* metabolizers (IM; carriers of *UGT1A1**60 or homozygous variant *UGT1A1**28) relative to normal metabolizers (NM; no copies of *UGT1A1**60 and one or fewer copies of *UGT1A1**28) [5].

In this same clinical trial, there was a significant ($p=0.0081$) correlation between the number of variant *UGT1A1* alleles (from zero to four variant alleles involving both *28 and *60) and the incidence of grade 3–4 thrombocytopenia (platelet nadir below 75,000/ μ L) relative to grades 0–2 [6]. This correlation was hypothesized to be related to variant *UGT1A1* alleles reducing belinostat clearance and, therefore, increasing drug exposure. This drug-induced reduction in circulating platelets (thrombocytes) has been observed in several other HDI therapies, including abexinostat [7, 8], panobinostat [9], romidepsin [10–12], and vorinostat [13], and has been hypothesized to be caused by a prolongation in the platelet precursor megakaryocyte maturation [14]. In this brief report, we expand upon this aforementioned PPK model, adding a semi-mechanistic myelosuppression pharmacodynamic (PD) model for the reduction in circulating platelets to better understand the exposure/response relationship between belinostat and platelets.

Methods

The study design and other details of this trial (NCT00926640) have been previously reported [4–6]. This trial was approved by the Institutional Review Board of the National Cancer Institute, and informed consent was obtained from all patients enrolled (Table S1). PK sampling occurred during cycle 1 at several time points during the 48-h continuous intravenous infusion, as well as up to 12-h post-end of infusion; all samples were measured using a validated uHPLC-MS/MS assay with a calibration range of 5–1500 ng/mL (see [5] for full details). Platelet counts were obtained at several points throughout cycle 1, per protocol-mandated patient monitoring. All patients enrolled on this study were genotyped for *UGT1A1*, as described previously [4–6].

A two compartment PPK model utilizing non-linear mixed-effects (NLME) modeling with a proportional residual error model and accounting for samples below assay quantitation limits with the M3 method was developed and validated using Phoenix[®] NLME 1.3 (Certara, Cary, NC,

USA) that utilized the Laplacian algorithm for determining the objective function value, as previously described [5]. Significant covariates were albumin, creatinine clearance, and *UGT1A1* genotype status (IM vs NM) on the clearance parameter, and body weight on the central volume parameter.

Upon including the platelet count data, a semi-mechanistic myelosuppression PD model was incorporated into the fixed PPK model based on previously published drug-induced thrombocytopenia models [7, 8, 15]. The PD portion of the model incorporated proliferation, maturation, and circulation compartments for platelets, as well as a feedback mechanism to avoid overproduction during the rebound effect. Structural parameters from the PD model included baseline levels of circulating platelets (Base), the drug effect on platelet decrease (Slope), the exponent of the feedback mechanism (Gamma), and rate constants for the megakaryocyte proliferation rate (k_{PROL}), initial transit rate (k_{PT}), inter-maturation compartment transit rate (k_{TR}), and degradation of platelets (k_{DEG}) (Supplemental Figure S1). The model-predicted circulating platelets levels (Circ) were based on observed (measured) platelet levels and a proportional residual error model.

The PPK/PD base model was developed in a stepwise manner and the likelihood ratio test used to determine the optimal model from nested comparisons. Several covariates were available from this data set, including sex, age, body weight, height, body surface area, *UGT1A1* genotype, renal function, albumin, and various liver function tests. Each covariate was explored for a potential influence on the PD parameters (covariates were already fixed into the PPK model). A visual predictive check (VPC; $n=500$ replicates) was run to visualize confidence intervals around model-predicted circulating platelet levels with binning at explicit centers at 0-, 12-, 36-, 48-, 60-, 72-, 144-, 168-, 225-, 250-, 325-, 400-, 475-, 550-, and 600-h post-dose. Standard errors and 95% confidence intervals were obtained through internal validation via nonparametric bootstrap ($n=500$ replicates).

To perform simulations, albumin, body weight, sex (binary: M or F), *UGT1A1* genotype (binary: IM or NM), serum creatinine, age, and creatinine clearance were randomly generated for 30 simulated subjects using Rv3.4.2 (<http://www.R-project.org>). Age, body weight, sex, and serum creatinine were needed to generate simulated CRCL using the Cockcroft–Gault method. Albumin, genotype, and creatinine clearance (CRCL) were covariates on the clearance parameter, while body weight was a covariate on central volume. These 30 simulated subjects were divided into five dose levels ($n=6$ per dose level): 250, 300, 400, 500, and 600 mg/m² administered as a 48-h IV infusion. The PK portion of the model remained fixed, while the PD portion was allowed to vary between subjects based on model-predicted inter-individual variability. Model-predicted belinostat plasma concentrations were simulated for the first

60 h following a dose, while model-predicted circulating platelet levels were simulated at all time points (every hour) for the entire 21-day cycle. A total of four cycles of therapy were simulated to assess the cumulative impact of increasing belinostat exposure on circulating platelet levels.

Unpaired group comparisons were performed using the nonparametric (due to low sample size) Mann–Whitney test. Comparisons between nested models were made using the Chi-squared test (Phoenix NLME®). Correlations between two continuous variables used the nonparametric Spearman correlation. Linear regression was used to analyze the relationship between belinostat exposure and platelet levels. All statistical tests (aside from Chi-squared test) were performed using GraphPadPrism, v7.01.

Results

Twenty-three patients on this trial had sufficient PK, genotype, and platelet data for inclusion in this modeling exercise. Patients categorized as IM not only had slower belinostat plasma clearance [5, 6], but also tended to have a lower platelet nadir vs NM [41,800 ($n=18$) vs 70,400 ($n=5$) count/ μL ; $p=0.053$ (Mann–Whitney); Supplemental Figure S2] that occurred roughly 6–7 days after cessation of belinostat. Based on this observation that slower belinostat clearance induced greater platelet decrease, coupled with an overall decrease in platelets with increasing belinostat concentration (Supplemental Figure S3), a semi-mechanistic myelosuppression PD model that included a rate constant between the proliferating and first maturation compartment (k_{PT}) was added onto the original PPK model [5]. This differed from comparable models that used the same rate constant for this process as well as the inter-maturation compartment transit rate constant [k_{TR} ; calculated by mean transit time (MTT) = $4/k_{\text{TR}}$, with MTT as an estimable parameter], which was assumed equivalent to k_{DEG} and k_{PROL} at steady state [7, 8, 15]. The k_{PT} rate constant was necessary for this

model to capture the data as k_{PT} proved a much slower process than k_{TR} (Table 1). Without k_{PT} , the model was wildly unpredictable of observed data, particularly the platelet recovery.

Based on the lower platelet nadir trend in IM, it was hypothesized that *UGT1A1* genotype impacted the drug effect on platelets; however, only a very minor, nonsignificant increase in Slope was seen in IM vs NM (not shown). Furthermore, random effects on Slope were not included in the final model due to eta shrinkage >0.9 , indicating insufficient population information (due to sparse platelet measurements during cycle 1) to accurately describe inter-individual variability (IIV); only Base and Gamma were allowed to vary between individuals. The rate constants (k_{PROL} , k_{PT} , k_{TR} , and k_{DEG}) all described the physiological processes involving platelet maturation, and thus, estimating IIV on these parameters would unnecessarily complicate the model.

There were several covariates that appeared to influence Base and Gamma, namely sex and *UGT1A1* genotype (Supplemental Figure S4). Males and NM tended to have higher baseline platelet counts compared to females and IM. These trends were also nearly identical on the Gamma parameter, due to the strong covariance (Spearman $\rho=0.879$) between etaBase and etaGamma when using a variance–covariance block matrix. Increasing albumin levels also appeared to be slightly correlated with increasing Base, which supports physiological evidence that suggests lower amounts of albumin lead to platelet aggregation, hence depletion of circulating platelets [16] that could lead to thrombocytopenia [17]. Although these trends were clear and improved the model when included as covariates, the improvement in the model did not warrant inclusion in the final model ($0.01 < p < 0.05$). To further support including no covariates, backward elimination of each covariate did not significantly worsen the model beyond acceptable criteria ($p < 0.005$; Chi-square test) and IIV for that parameter did not improve by 25% or more. Therefore, no covariates were included in the final PD portion of the model; however, the base model

Table 1 Estimable pharmacodynamic model parameters

Parameter	Point estimate (%CV)	Bootstrap estimate (%CV) ¹	Bootstrap 95% CI
Kprol (1/min)	0.446 (0.867%)	0.517 (26.8%)	0.390–0.888
Kdeg (1/min)	0.471 (2.42%)	0.483 (6.47%)	0.432–0.558
Ktr (1/min)	119.9 (1.94%)	122.5 (11.8%)	96.96–158.9
Kpt (1/min)	0.584 (0.806%)	0.639 (27.9%)	0.378–1.13
Slope (L/mg)	0.15178 (0.971%)	0.1479 (28.5%)	0.079–0.212
Base (ct/mL)	175.71 (1.13%)	173.16 (3.17%)	155.2–178.6
IIV base (%)	20.1 (0.003%)	20.4 (0.08%)	N/A
Gamma	0.5674 (1.78%)	0.4566 (35.8%)	0.0319–0.6219
IIV Gamma (%)	26.7 (0.004%)	23.9 (0.16%)	N/A
ρ_{COV} (Base,Gamma)	0.8792	0.7555	N/A
RUV (%)	38.07 (0.678%)	36.72 (8.32%)	29.9–42.3

still adequately described the observed platelet data based on model diagnostics (Supplemental Figure S5A–B) and a visual predictive check ($n = 500$ replicates) (Fig. 1a).

Simulations over the first cycle of therapy (days 1–21) demonstrated that the lowest simulated dose level (250 mg/m²) had a mean predicted platelet nadir of ~60,000/ μ L (grade 2) occurring on the 8th day post-therapy start, whereas the highest dose level (600 mg/m²) had a mean predicted nadir of ~40,000/ μ L (grade 3) that occurred on the 10th day post-dose. It was predicted that while lower dose levels of belinostat can result in thrombocyte nadirs below 75,000/ μ L (qualifying as a moderate grade 2 event), the duration is short-lived and platelet levels quickly rebound above 100,000/ μ L within another 48 h. The 600-mg/m² dose level was predicted to reach grade 3 levels (25,000–50,000/ μ L) by 6-day post-therapy start and remain below 75,000/ μ L

for another week. Eventually, all dose levels were predicted to return mean platelet levels back to baseline by day 21, just prior to the start of the next dose (Fig. 1b). Therefore, no cumulative effect on platelet levels by belinostat, and possibly belinostat + cisplatin + etoposide, was evident with repeated q21day dosing.

Discussion

Several HDIs have been shown to decrease thrombocyte count, including abexinostat [7, 8], panobinostat [9], romidepsin [10–12], and vorinostat [13]. Goey et al. demonstrated that patients with an IM status for *UGT1A1* (i.e., greater belinostat exposure) had greater incidence of grade 3 (platelet count between 25,000–50,000/ μ L) or grade 4 (<25,000/ μ L) thrombocytopenia compared to NM when receiving the belinostat, cisplatin, and etoposide combination [6]. This was consistent with IMs having a slower belinostat clearance and thus the recommendation of a 33% dose reduction for IMs based on PPK modeling and simulation when giving belinostat as a 48-h IV infusion [5].

This report sought to describe the mechanism relating the PPK of belinostat to thrombocytes to model an exposure/response relationship, and describe platelet depletion and recovery over the course of the first cycle of therapy. While belinostat was infused over 48 h, the platelet nadir occurred around 8 days before mostly recovering back to pre-treatment levels around 19–20-day post-therapy. In this study, belinostat was infused every 21 days in addition to concomitant cisplatin and etoposide that could also have contributed to thrombocyte depletion. Goey et al. suggested that because *UGT1A1* genotype was so highly correlated with grade of thrombocytopenia, in this regimen, it is possible that belinostat exposure played a more predominant role relative to cisplatin and/or etoposide [6]. To simplify this model, we focused only on the contribution of belinostat on platelets, specifically the mechanism of delayed maturation of megakaryocytes. Ultimately, *UGT1A1* genotype status was not shown to be a significant predictor of thrombocytopenia based on the lack of model improvement when this variable was added as a covariate, likely due to insufficient population information on the most relevant parameter (Slope; eta shrinkage > 0.9). However, the genotype effect was evident as measured by a lower platelet nadir in IM vs NM.

Plotting the simulated results based on *UGT1A1* genotype did not demonstrate any differences in platelet changes during a simulated 21-day cycle. This is consistent with the nonsignificant change in the Slope parameter between IM and NM, prior to removing IIV on Slope due to high eta shrinkage. This suggests that the model did not have enough data (only a single cycle of data from 23 patients) to make accurate predictions on the covariate effects on IIV on the

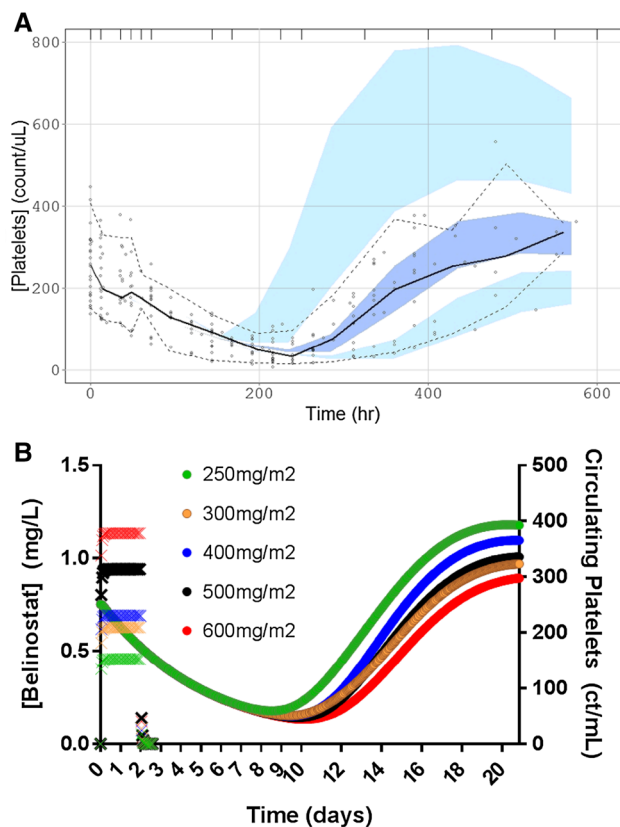


Fig. 1 PPK/PD goodness-of-fit plots. **a** Visual predictive check performed 500 times with the 5th, 50th (median), and 95th prediction intervals was calculated around each observed 5th, 50th, and 95th quantile. **b** Simulation results of five dose levels (250, 300, 400, 500, and 600 mg/m²), with $n = 6$ simulated patients within each dose level over the course of one cycle of therapy. The left y-axis represents the belinostat plasma concentrations (“x” symbols) for each dose level. The steady-state levels during the 48-h IV infusion are evident, but the elimination phase is not as much due to the limited x-axis space. For a better depiction of belinostat elimination kinetics, refer to [5]. The simulated platelet levels are depicted in the right y-axis and with “o” symbols

Slope parameter. It is likely that there may be a *UGT1A1* genotype effect on Slope, but this data set did not have enough observed data to identify one. However, the framework of the model described here allows for future inclusion of *UGT1A1* genotype as a covariate on Slope.

The previous models of HDI-induced thrombocytopenia have described a slight overcompensation of thrombocyte recovery following depletion of platelet counts (rebound effect) [7, 8]. In this data set, a similar rebound effect was evident in observable data, and the model mostly reflected that based solely on cycle 1 data (Fig. 1b). In addition, it was shown that HDI-mediated decreases in platelets are largely dependent on the drug administration schedule over a cycle, and for a drug with a short half-life like abexinostat (4 h), administration over a 2–4-day period of a 3-week cycle resulted in the best safety profile [7]. Repeated dosing on further cycles led to an attenuation of platelet decreases as progenitor cells had been previously stimulated (characterized by k_{PROL}) from the prior treatment cycle [7]. This leads to a flattening out of platelet counts with repeated cycles of therapy until cessation of treatment, and simulations performed in this study are consistent with this through four cycles of therapy.

In conclusion, the model presented here adequately describes the exposure/response relationship between belinostat plasma levels and the resulting circulating platelet count. However, this model suggests that the effect of *UGT1A1* genotype status (NM vs IM) did not result in significantly different rates of platelet decreases, or at the least this data set had insufficient observations to accurately predict any differences. Rather, this model showed a belinostat plasma concentration-dependent decrease of platelets based on increasing dose, as well as an influence on the duration of platelet decrease (delay in rebound effect). Additional data will only help to improve the ability of this model to predict changes in platelets during this therapeutic regimen, especially regarding *UGT1A1* genotype status as a potential diagnostic marker. This information may be useful in determining the time course of occurrence of thrombocytopenia and possibly which patients (e.g., based on *UGT1A1* genotype) may be more greatly affected.

Acknowledgements We thank all of the nurses and clinical support staff for their patient care, the Blood Processing Core of the NCI for their sample handling/processing. The content of this publication does not necessarily reflect the views or policies of the Department of Health and Human Services, nor does mention of trade names, commercial products, or organizations imply endorsement by the US Government.

Funding This project has been funded in whole or in part with federal funds from the National Cancer Institute, National Institutes of Health. This work was supported by the Intramural Research Program of the NIH, National Cancer Institute, Center for Cancer Research (Grant # ZIC BC 010548).

Compliance with ethical standards

Conflict of interest Author CJP declares that he has no conflict of interest. OMH declares that he has no conflict of interest. TMS declares that he has no conflict of interest. RP declares that he has no conflict of interest. SB declares that he has no conflict of interest. SEB declares that she has no conflict of interest. WDF declares that he has no conflict of interest.

Ethics approval All clinical data presented in this manuscript was obtained from a clinical trial (NCT 00926640) that was approved by the IRB of the National Cancer Institute. All procedures performed in studies involving human participants were in accordance with the ethical standards of the institutional and/or national research committee and with the 1964 Helsinki declaration and its later amendments or comparable ethical standards.



Informed consent Informed consent was obtained from all individual participants included in the study.

References

1. Thomas A, Rajan A, Szabo E et al (2014) A phase I/II trial of belinostat in combination with cisplatin, doxorubicin, and cyclophosphamide in thymic epithelial tumors: a clinical and translational study. *Clin Cancer Res* 20:5392–5402
2. Luchenko VL, Salcido CD, Zhang Y et al (2011) Schedule-dependent synergy of histone deacetylase inhibitors with DNA damaging agents in small cell lung cancer. *Cell Cycle* 10:3119–3128
3. Kim MS, Blake M, Baek JH et al (2003) Inhibition of histone deacetylase increases cytotoxicity to anticancer drugs targeting DNA. *Cancer Res* 63:7291–7300
4. Balasubramaniam S, Redon CE, Peer CJ et al (2018) Phase I trial of belinostat with cisplatin and etoposide in advanced solid tumors, with a focus on neuroendocrine and small cell cancers of the lung. *Anticancer Drugs* 29:457–465
5. Peer CJ, Goey AK, Sissung TM et al (2015) *UGT1A1* genotype-dependent dose adjustment of belinostat in patients with advanced cancers using population pharmacokinetic modeling and simulation. *J Clin Pharmacol* 56:450
6. Goey AK, Sissung TM, Peer CJ et al. (2015) Effects of *UGT1A1* genotype on the pharmacokinetics, pharmacodynamics and toxicities of belinostat administered by 48 h continuous infusion in patients with cancer. *J Clin Pharmacol* 56:461
7. Chalret du Rieu Q, Fouliard S, Jacquet-Bescond A et al (2013) Application of hematological toxicity modeling in clinical development of abexinostat (S-78454, PCI-24781), a new histone deacetylase inhibitor. *Pharm Res* 30:2640–2653
8. Fouliard S, Robert R, Jacquet-Bescond A et al (2013) Pharmacokinetic/pharmacodynamic modelling-based optimisation of administration schedule for the histone deacetylase inhibitor abexinostat (S78454/PCI-24781) in phase I. *Eur J Cancer* 49:2791–2797
9. Younes A, Sureda A, Ben-Yehuda D et al (2012) Panobinostat in patients with relapsed/refractory Hodgkin's lymphoma after autologous stem-cell transplantation: results of a phase II study. *J Clin Oncol* 30:2197–2203
10. Piekarz RL, Frye R, Turner M et al (2009) Phase II multi-institutional trial of the histone deacetylase inhibitor romidepsin as monotherapy for patients with cutaneous T-cell lymphoma. *J Clin Oncol* 27:5410–5417

11. Grant C, Rahman F, Piekarz R et al (2010) Romidepsin: a new therapy for cutaneous T-cell lymphoma and a potential therapy for solid tumors. *Expert Rev Anticancer Ther* 10:997–1008
12. Piekarz RL, Frye R, Prince HM et al (2011) Phase 2 trial of romidepsin in patients with peripheral T-cell lymphoma. *Blood* 117:5827–5834
13. Duvic M, Talpur R, Ni X et al (2007) Phase 2 trial of oral vorinostat (suberoylanilide hydroxamic acid, SAHA) for refractory cutaneous T-cell lymphoma (CTCL). *Blood* 109:31–39
14. Bishton MJ, Harrison SJ, Martin BP et al (2011) Deciphering the molecular and biologic processes that mediate histone deacetylase inhibitor-induced thrombocytopenia. *Blood* 117:3658–3668
15. Sasaki T, Takane H, Ogawa K et al (2011) Population pharmacokinetic and pharmacodynamic analysis of linezolid and a hematologic side effect, thrombocytopenia, in Japanese patients. *Antimicrob Agents Chemother* 55:1867–1873
16. Mikhailidis DP, Ganotakis ES (1996) Plasma albumin and platelet function: relevance to atherogenesis and thrombosis. *Platelets* 7:125–137
17. Bautista MJ, Ruiz-Villamor E, Salguero FJ et al (2002) Early platelet aggregation as a cause of thrombocytopenia in classical swine fever. *Vet Pathol* 39:84–91

Affiliations

Cody J. Peer¹  · Oliver M. Hall¹ · Tristan M. Sissung¹ · Richard Piekarz² · Sanjeeve Balasubramaniam³ · Susan E. Bates⁴ · William D. Figg^{1,5} 

Cody J. Peer
cody.peer@nih.gov

Oliver M. Hall
oliver.hall@nih.gov

Tristan M. Sissung
sissung@mail.nih.gov

Richard Piekarz
piekarzr@mail.nih.gov

Sanjeeve Balasubramaniam
sanjeeve.balasubramaniam@fda.hhs.gov

Susan E. Bates
seb2227@cumc.columbia.edu

¹ Clinical Pharmacology Program, CCR, National Cancer Institute, NIH, 10 Center Drive, Room 5A01, Bethesda, MD 20892, USA

² Cancer Therapy Evaluation Program, National Cancer Institute, NIH, Bethesda, MD 20892, USA

³ Office of Hematology Oncology Products, US Food and Drug Administration, Silver Spring, MD 20993, USA

⁴ Department of Hematology and Oncology, Columbia University Medical Center, New York, NY 10032, USA

⁵ Genitourinary Malignancies Branch, National Cancer Institute, NIH, Bethesda, MD 20892, USA